Pattern Formation in Systems with Multiple Delayed Feedbacks

Serhiy Yanchuk[1] and Giovanni Giacomelli[2]
[1]Institute of Mathematics, Humboldt University of Berlin, Unter den Linden 6, 10099 Berlin, Germany
[2]CNR-Istituto dei Sistemi Complessi-via Madonna del Piano 10, I-50019 Sesto Fiorentino (FI), Italy
(Received 18 January 2014; revised manuscript received 14 March 2014; published 2 May 2014)

Dynamical systems with complex delayed interactions arise commonly when propagation times are significant, yielding complicated oscillatory instabilities. In this Letter, we introduce a class of systems with multiple, hierarchically long time delays, and using a suitable space-time representation we uncover features otherwise hidden in their temporal dynamics. The behavior in the case of two delays is shown to "encode" two-dimensional spiral defects and defects turbulence. A multiple scale analysis sets the equivalence to a complex Ginzburg-Landau equation, and a novel criterium for the attainment of the long-delay regime is introduced. We also demonstrate this phenomenon for a semiconductor laser with two delayed optical feedbacks.

DOI: 10.1103/PhysRevLett.112.174103 PACS numbers: 05.45.-a, 02.30.Ks, 89.75.Kd

Systems with time delays are common in many fields, including optics (e.g., a laser with feedback [1–4]), vehicle systems [5], neural networks [6], information processing [7], and many others [8]. A finite propagation velocity of the information introduces in such systems a new relevant scale, which is comparable or higher than the intrinsic time scales. It has been shown that the complexity of such systems, e.g., the dimension of attractors, is finite and it grows linearly with time delay [9]; moreover, the spectrum of Lyapunov exponents approaches a continuous limit for a long delay [10–12]. As a result, in this case essentially high-dimensional phenomena can occur such as spatiotemporal chaos [13], square waves [8], Eckhaus destabilization [14], or coarsening [3]. In the above mentioned situations, the system involves one long delay, which can be interpreted as the size of a one-dimensional, spatially extended system [13,15]. This approach has proven to be instrumental in explaining new phenomena in systems with time delays [16,17].

In this Letter, we show that many new challenging problems arise when a system is subject to several delayed feedbacks acting on different scales. In contrast to the single delay situation, essentially new phenomena occur, related to higher spatial dimensions involved in the dynamics, such as spirals or defect turbulence. As an illustration, we consider a specific physical system, namely, a model of a semiconductor laser with two optical feedbacks.

A simple paradigmatic setup for the multiple delays case is the following system:

$$\dot{z} = az + bz_{\tau_1} + cz_{\tau_2} + dz|z|^2. \tag{1}$$

Equation (1) describes a very general situation: the interplay of the oscillatory instability (Hopf bifurcation) and two delayed feedbacks $z_{\tau_i} = z(t-\tau_i)$, which we consider acting on different time scales $1 \ll \tau_1 \ll \tau_2$. The variable $z(t)$ is complex, and the parameters a, b, and c determine the instantaneous τ_1-and τ_2-feedback rates, respectively. The instantaneous part of the system (without delayed feedback) is known as the normal form for the Hopf bifurcation.

The following basic questions arise: What kind of new phenomena can be observed in systems with several delayed feedbacks? Can one relate the dynamics of such systems to spatially extended systems with several spatial dimensions? In the case of positive answer, under which conditions? Is it possible to observe such essentially 2D phenomena as, e.g., spiral waves in purely temporal delay systems, Eq. (1), which obey the causality principle with respect to the time? In this Letter, we address the above questions. In particular, we show that such inherently 2D patterns as spiral defects or defect turbulence [18] are typical behaviors of the system in Eq. (1). Moreover, they can be generically found in a semiconductor laser model with two optical feedbacks.

We start with numerical examples. Figures 1 and 2 show solutions of Eq. (1) for two different parameter choices. The time series in Figs. 1(a) and 2(a) exhibit oscillations on different time scales related approximately to the delay times. However, an appropriate spatiotemporal representation of the data [see e.g., Figs. 1(b)–1(c) and 2(b)–2(c)] reveals clearly the nature of the dynamical behaviors. More details on the appropriate spatiotemporal representation of these purely temporal data will be given later, but one can readily observe that the first case corresponds to a (frozen) spiral (FS) defects solution, see Figs. 1(b) and 1(c). The positions of the two coexisting spiral defects are shown by the dots, where the level lines for the phase meet. Consequently, the phase is not defined there and $|z| = 0$. The solution shown in Fig. 2 corresponds instead to the defect turbulence (DT) regime. One can observe that the

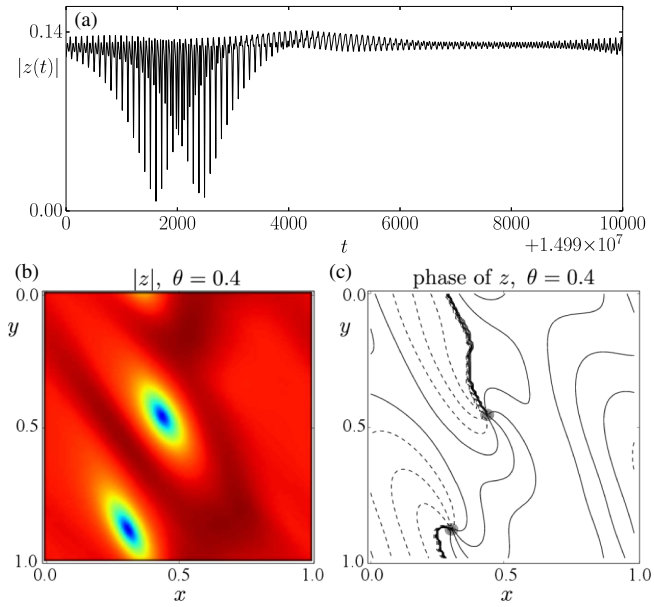

FIG. 1 (color online). Spiral defects in a system with delays, Eq. (1). (a) Typical time series of the absolute value $|z(t)|$. Spatiotemporal representation of the time series using pseudospace coordinates, Eq. (3), reveals the spiral defects: (b) Snapshot of the spatial profile in the pseudospace coordinates (x, y) for $\theta_0 = 0.4$. (c) Constant level lines for the phase of z. Circles denote the positions of defects. Parameters: $a = -0.985$, $b = 0.4$, $c = 0.6$ (corresponding to $P = 0.015$), $d = -0.75 + i$, $\tau_1 = 100$, and $\tau_2 = 10\,000$. Initial conditions are chosen randomly. See the Supplemental Material [19] for the dynamics of the patterns.

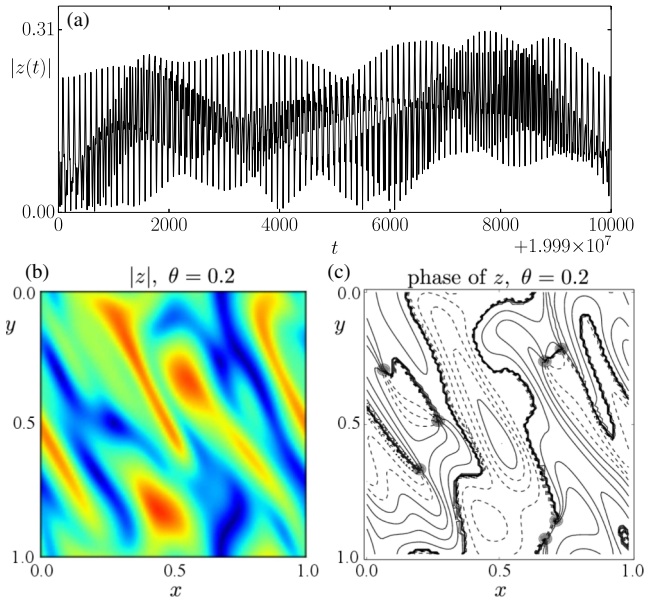

FIG. 2 (color online). Defects turbulence in delayed system, Eq. (1). Same as in Fig. 1 for a different value of $d = -0.1 + i$. Spatiotemporal representation in (b) and (c) reveals defects turbulence.

modulation of the amplitude $|z(t)|$ starts to approach the zero level in a randomlike manner. In this case, the corresponding spatial representation [see Figs. 2(b) and 2(c)] reveals DT, i.e., the nonregular motions of the spiral defects. The plots correspond to snapshots in time; the videos in the Supplemental Material [19] show the temporal dynamics of those patterns.

In the following, we explain why the observed behaviors are typical and show how to relate the dynamics of Eq. (1) to the complex Ginzburg-Landau equation on a 2D spatial domain. In particular, we show that the function $z(t)$ on the time interval of the length τ_2 corresponds to a snapshot of a 2D *spatial* function $\Phi(x, y)$. The corresponding pseudospatial coordinates x and y introduced later by Eq. (3) are different scales of the time. We will show that the parameters of Eq. (1) leading to the FS (respectively, DT) can be mapped uniquely to the parameters of the Ginzburg-Landau system, for which the same phenomenologies are observed [18]. This behavior is observed robustly for all tested random initial conditions for an interval of parameters.

Normal form equation.— The long time delay τ_1 can be written as $\tau_1 = 1/\varepsilon$ with a small positive parameter ε, and $\tau_2 = \kappa/\varepsilon^2$ with some positive κ. With such notations, the scale separation $1 \ll \tau_1 \ll \tau_2$ is satisfied. Notice that this also gives an indication of how one should proceed in the case of more than two delays.

In order to derive a normal form describing universally the dynamics close to the destabilization of the system in Eq. (1), the multiple scale ansatz $z(t) := \varepsilon u(\varepsilon t, \varepsilon^2 t, \varepsilon^3 t, \varepsilon^4 t)$ is used. More precisely, substituting this ansatz as well as the perturbation parameter $\varepsilon^2 p = a + |b| + |c|$ in Eq. (1), and time delays $\tau_1 = 1/\varepsilon$, $\tau_2 = \kappa/\varepsilon^2$, one obtains several separate solvability conditions for different orders of ε [see the Supplemental Material [19] for more details]. The resulting equation is the Ginzburg-Landau partial differential equation,

$$\Phi_\theta = p\Phi + a_1\Phi_x + a_2\Phi_y + a_3\Phi_{xx} + a_4\Phi_{xy} + a_5\Phi_{yy} + d\Phi|\Phi|^2, \tag{2}$$

for a function $\Phi(\theta, x, y)$, which is related to the solutions of Eq. (1) by $z(t) = \varepsilon\Phi(\theta, x, y)$, where

$$\theta = \varepsilon^4\delta t, \qquad x = \varepsilon t(1 - \delta\varepsilon^2), \qquad y = \varepsilon^2 t(1 - |b|\delta\varepsilon), \tag{3}$$

and $\delta = -(a + |b|)^{-1} > 0$. The new spatial variables x and y are different time scales of the original time t, and the new time variable θ is the slow time scale $\varepsilon^4 t$. Therefore, the new spatial and temporal variables can be called pseudospace and pseudotime. The coefficients in Eq. (2) are $a_1 = a_4 = \delta|b|$, $a_2 = -1 + \delta|b|^2$, $a_3 = \delta/2$, and $a_5 = -\delta a|b|/2$. One can note that the diffusion coefficients in this equation are real. The dynamics of Eq. (2) is known

[18,24] to possess various phase transitions, FS (e.g., for $d = -0.75 + i$), and DT (e.g., for $d = -0.1 + i$). We found a good correspondence between the dynamics of the systems in Eqs. (2) and (1), taking into account the relation to Eq. (3) between them. Although a systematic parametric investigation is out of the scope of this Letter, the examples of FS and DT for the above mentioned parameter values shown in Figs. 1 and 2 are well reproduced. Moreover, the observed dynamics is robust with respect to small variations of parameters. We remark that the observed phenomena are not possible in systems with one time delay, since they arise from the two-dimensional space (x, y) of the normal form equation.

Drift and comoving Lyapunov exponents.— The spatial coordinates in Eq. (3) can be rewritten as $x = \bar{x} - \delta\bar{u}$ and $y = \bar{y} - |b|\delta\bar{u}$, where $\bar{x} = \varepsilon t$, $\bar{y} = \varepsilon^2 t$ and $\bar{u} = \varepsilon^3 t$. As a consequence, we can infer the existence of a (fast) drift along the vector $\mathbf{V}_d = (-1, -|b|)$ in the "naïve" coordinates $(\bar{x}, \bar{y})$. The corrected coordinates in Eq. (3) eliminate this drift so that the remaining variables are governed by the Ginzburg-Landau Equation (2).

The above phenomenon is a consequence of the properties of the maximal comoving (or convective) Lyapunov exponent Λ [25]. In the spherical coordinates $\bar{u} = \rho\cos\alpha$, $\bar{y} = \rho\sin\alpha\cos\beta$, $\bar{x} = \rho\sin\alpha\sin\beta$, it is found that

$$\Lambda(\alpha,\beta) = a\sin\alpha\sin\beta + (1 + \log(|b|\tan\beta))\sin\alpha\cos\beta + (1 + \log(|c|\sin\beta\tan\alpha))\cos\alpha. \quad (4)$$

Details of the calculation will be presented elsewhere. A geometrical interpretation can be introduced using the velocity $\mathbf{V} = (\sin\beta\tan\alpha, \cos\beta\tan\alpha)$, along which the perturbations evolve with a multiplier $e^{\Lambda(\alpha,\beta)}$. The propagation cone's boundaries can be defined as the set (α, β) such that $\Lambda(\alpha,\beta) = 0$. The bifurcation point, attained when the maximum of Λ is equal to zero, is obtained at $\mathbf{V} = \delta\mathbf{V}_d$, corresponding to $(\alpha_0,\beta_0) = (\tan^{-1}(-\delta\sqrt{1+|b|^2})\tan^{-1}(|b|^{-1}))$. Note that the direction $\mathbf{V}_d$ is also given by the multiscale method above. The above result extends the standard linear stability analysis by indicating the direction along which the destabilization takes place. We notice that the comoving exponent diverges logarithmically close to the axis $\alpha = 0$ and $\beta = 0$; i.e., instantaneous propagations are forbidden. In the opposite limit, $\alpha \to \pi/2$ (respectively, $\beta \to \pi/2$); Λ approaches the value for the single delay case $c = 0$ $(b = 0)$. Finally when both $\alpha, \beta \to \pi/2$ (infinite velocity), $\Lambda = a$ and the dynamics is governed by the local term as expected.

On the long-delay approximation.— Concerning the relation between the delay system, Eq. (1), and the normal form in Eq. (2), the following questions arise: To what extent is the equivalence founded? Under which conditions are the delays large "enough"? Dynamically, the absence of the anomalous Lyapunov exponents [10] is required, or, equivalently, the absence of strong chaos [11]. Numerically, with the decreasing of delays, the spatiotemporal structures become transients towards a periodic or constant amplitude ($|z| = \text{const}$) state. As a matter of fact, a solution of the delay system evolves along the one-parametric line $(\theta(t), x(t), y(t))$ defined by Eq. (3) in the pseudospace (θ, x, y); see Fig. 3(a). In order to have a good correspondence between the solutions of the delay system, Eq. (1), and the normal form through the parametrization, Eq. (3), the line $(x(t), y(t))$ should wind up in the space (x, y) sufficiently densely. In the leading order, this line satisfies $y \approx \varepsilon x$ and it is wrapped periodically at $x = 0$ and $x = 1$; see Fig. 3(a). The distance between the neighboring branches is $\sim\varepsilon$ which determines the "discretization" level. Thus, high delays imply a dense covering of the (pseudo) space plane, as expected in the thermodynamic limit. However, when such density is too small, the dynamics changes drastically and the delay system behaves quite differently from the corresponding normal form.

To illustrate such a behavior, we present in Fig. 3(b) the analysis of the amplitude $|z|$ statistics in the defect turbulence regime for the model, Eq. (1). For small delays, the dynamics relaxes to a stationary oscillating regime after a transient, with the corresponding histogram showing a shape very close to that obtained from a sinusoidal signal. For higher τ's , the histogram starts displaying a power-law tail $P(|z|) \sim |z|^1$ for $|z| \to 0$, indicating the stable appearance of defects and the attainment of the long-delayed regime.

The scaling exponent can be obtained analytically for an arbitrary number of delays and equations. In the DT regime, defects are the spatial points where $|\Phi| = 0$ in an N-dimensional space (N being the number of delays) and

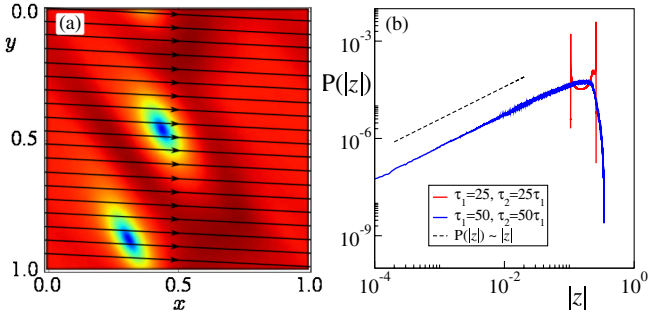

FIG. 3 (color online). "Small" delays effect. (a) One-parameter curve $x(t)$, $y(t)$ in the pseudospace determined by Eq. (3) for $\varepsilon = 0.05$. For larger distances between the branches (smaller delays), the line does not resolve the cores of the spiral of the corresponding Ginzburg-Landau model. (b) Numerical histograms of $|z|$ for the DT regime (parameters as in Fig. 2) for increasing the delays values. Histograms for smaller delays (here, $\tau_1 = 25$, $\tau_2 = 25\tau_1$) correspond to bounded, periodic solutions with no defects, reached after a transient. A tail in the distribution appears for higher delays (here, $\tau_1 = 50$, $\tau_2 = 50\tau_1$). The dashed line is a reference curve $P(|z|) \sim |z|^1$.

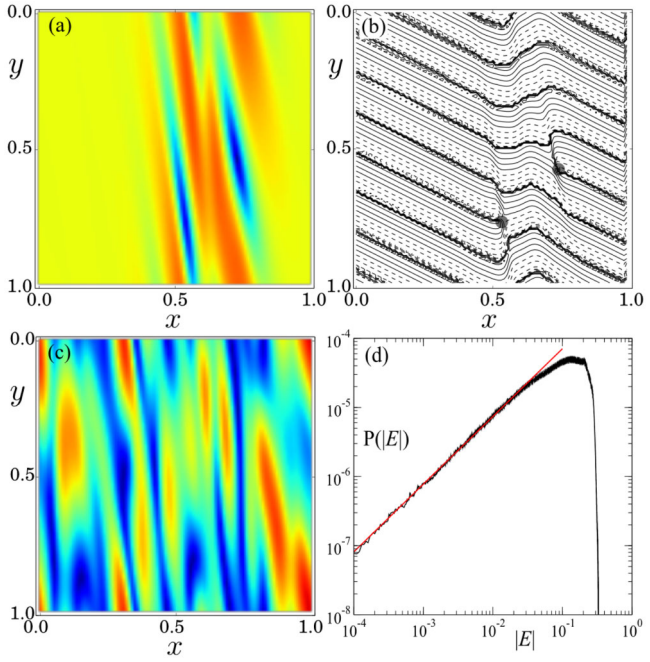

FIG. 4 (color online). Dynamics of the solution E of the system in Eq. (5), represented as snapshot in the pseudospace for the parameter values: $\tau_1 = 10^2$, $\tau_2 = 10^4$, $\eta_1 = \eta_2 = 0.1$, $T = 10^2$, and $J = -0.17$. (a), (b) Amplitude and phase of E for $\alpha = 2$, showing the occurrence of spiral defects. (c) Amplitude of E, defects turbulence regime for $\alpha = 4$. The temporal behavior is presented as movies in the Supplemental Material [19]. (d) Statistics of the field amplitude in the case (c); the line is a power-law fit of the tail with exponent 0.98.

form a set D that we can assume is of a constant density in space. In our case of $N = 2$, these are point defects, for $N = 3$ line defects, etc.. In general, it holds that $\mathrm{codim}(D) = 2$ in the N-dimensional space $\{x_1, x_2, \ldots, x_N\}$, where $\{x_i\}$ are pseudospatial coordinates. The delay equation(s) dynamics approaches D along the domain line $L = \{x_1(t), x_2(t), \ldots, x_N(t) : t \in \mathbb{R}\}$. The vicinity of defects in the pseudospace affects the amplitude statistics of the delay dynamics, which will be depending only on $\mathrm{codim}(D) = 2$ and on $\dim(L) = 1$. Thus, the scaling exponent does not depend on N or on the number of equations and it can be shown to be equal to 1.

Semiconductor laser with two optical feedbacks.— The results obtained from the study of the normal form, Eq. (1), are expected to apply to a wide class of physical systems. In the following, we consider a Lang-Kobayashi-type model [26] of a single mode semiconductor laser with optical feedback, generalized to a double external cavity configuration:

$$E'(t) = (1 + i\alpha)n(t)E(t) + \eta_1 E(t - \tau_1) + \eta_2 E(t - \tau_2),$$
$$Tn'(t) = J - n(t) - (2n(t) + 1)|E(t)|^2. \quad (5)$$

$E(t)$ is the complex electric field and $n(t)$ the excess carrier density. The system parameters are the excess pump current J, the external cavities round trip times τ_1 and τ_2 are measured in units of the photon lifetime, and the feedback strengths are η_1 and η_2. The linewidth enhancement factor α is specific for semiconductor lasers and affects many aspects of their behavior (see, e.g., [4]). We present here two examples of the dynamics of Eq. (5) in the case of $\alpha = 2$ and $\alpha = 4$. Suitable laser devices can be employed to realize the corresponding experiments; in fact, such a range is typical and, e.g., measurements in-between have been reported [27].

In our case, shortly after the destabilization of the "off-state" $E = 0$, a multifrequency oscillating behavior is found, corresponding to FS [$\alpha = 2$, Figs. 4(a)–4(b)] or DT [$\alpha = 4$, Fig. 4(c)]. These regimes are very similar to those shown in Fig. 1 and Fig. 2, respectively. In order to compare their statistical properties, we report also the distribution of the field amplitude $|E|$ [Fig. 4(d)]. Its shape is indeed consistent with the previous results and the scaling of the tail marks the sign of the long-delay regime as well. We point out also how α appears to be an effective parameter switching between just drifting defects [Figs. 4(a) and 4(b)] and irregularly moving defects [Fig. 4(c)], thus suggesting which kind of behavior could be expected for different laser devices.

In conclusion, we have discussed a class of systems describing the interplay of the oscillatory instability with multiple, hierarchically long, delayed feedbacks. We have shown that a generalized spatiotemporal representation is able to uncover multiscale features otherwise hidden in the complex temporal dynamics. In the case of two delays, the existence of regimes of FS and DT has been evidenced. By means of a multiple scale analysis, an equivalence is shown to a two-dimensional complex Ginzburg-Landau equation. The attainment of the long-delay regime has been also analyzed. Finally, we showed how the above phenomena occur in the case study of a semiconductor laser with two external cavity optical feedbacks, a generalization of a well-known and studied configuration. As a perspective, our approach can be applied in several experimental setups and in the study of higher-dimensional pattern formations in delay systems, such as the existence and characterization of line defects in the three delays case. Moreover, we expect that this formalism could be generalized for other types of bifurcations as well and applied to the study of specific experimental systems, such as delayed networks like those commonly found in optical communications.

We acknowledge the DFG for financial support in the framework of Collaborative Research Center (SFB) 910 and useful discussions with A. Politi.

[1] X. Li, A. B. Cohen, T. E. Murphy, and R. Roy, Opt. Lett. **36**, 1020 (2011).
[2] J. Zamora-Munt, C. Masoller, J. Garcia-Ojalvo, and R. Roy, Phys. Rev. Lett. **105**, 264101 (2010).
[3] G. Giacomelli, F. Marino, M. A. Zaks, and S. Yanchuk, Europhys. Lett. **99**, 58005 (2012).
[4] M. C. Soriano, J. García-Ojalvo, C. R. Mirasso, and I. Fischer, Rev. Mod. Phys. **85**, 421 (2013).
[5] R. Szalai and G. Orosz, Phys. Rev. E **88**, 040902 (2013).
[6] E. M. Izhikevich, Neural Comput. **18**, 245 (2006).
[7] L. Appeltant, M. C. Soriano, G. Van der Sande, J. Danckaert, S. Massar, J. Dambre, B. Schrauwen, C. R. Mirasso, and I. Fischer, Nat. Commun. **2**, 468 (2011).
[8] T. Erneux, *Applied Delay Differential Equations* (Springer, New York, 2009).
[9] J. D. Farmer, Physica (Amsterdam) **4D**, 366 (1982).
[10] G. Giacomelli, S. Lepri, and A. Politi, Phys. Rev. E **51**, 3939 (1995).
[11] S. Heiligenthal, T. Dahms, S. Yanchuk, T. Jüngling, V. Flunkert, I. Kanter, E. Schöll, and W. Kinzel, Phys. Rev. Lett. **107**, 234102 (2011).
[12] O. D'Huys, S. Zeeb, T. Jüngling, S. Heiligenthal, S. Yanchuk, and W. Kinzel, Europhys. Lett. **103**, 10013 (2013).
[13] G. Giacomelli and A. Politi, Phys. Rev. Lett. **76**, 2686 (1996).
[14] M. Wolfrum and S. Yanchuk, Phys. Rev. Lett. **96**, 220201 (2006).
[15] F. T. Arecchi, G. Giacomelli, A. Lapucci, and R. Meucci, Phys. Rev. A **45**, R4225 (1992).
[16] G. Giacomelli, R. Meucci, A. Politi, and F. T. Arecchi, Phys. Rev. Lett. **73**, 1099 (1994).
[17] L. Larger, B. Penkovsky, and Y. Maistrenko, Phys. Rev. Lett. **111**, 054103 (2013).
[18] H. Chaté and P. Manneville, Physica (Amsterdam) **224A**, 348 (1996).
[19] See the Supplemental Material at http://link.aps.org/supplemental/10.1103/PhysRevLett.112.174103 for details of the normal form derivation and movies illustrating the pattern dynamics, which includes Refs. [20–23].
[20] M. Wolfrum, S. Yanchuk, P. Hövel, and E. Schöll, Eur. Phys. J. Spec. Top. **191**, 91 (2010).
[21] S. Lepri, G. Giacomelli, A. Politi, and F. T. Arecchi, Physica (Amsterdam) **70D**, 235 (1994).
[22] S. Yanchuk and M. Wolfrum, SIAM J. Appl. Dyn. Syst. **9**, 519 (2010).
[23] M. Lichtner, M. Wolfrum, and S. Yanchuk, SIAM J. Math. Anal. **43**, 788 (2011).
[24] I. Aranson and L. Kramer, Rev. Mod. Phys. **74**, 99 (2002).
[25] R. J. Deissler and K. Kaneko, Phys. Lett. A **119**, 397 (1987).
[26] R. Lang and K. Kobayashi, IEEE J. Quantum Electron. **16**, 347 (1980).
[27] S. Barland, P. Spinicelli, G. Giacomelli, and F. Marin, IEEE J. Quantum Electron. **41**, 1235 (2005).